MULTI-SCALE APPROACH TO PREDICT THE ORTHOTROPIC ELASTICITY TENSOR OF CARBON FIBRES AND WOVEN CARBON COMPOSITES BY ULTRASONIC INSONIFICATION

R.D.B. Sevenois[1,2], S.W.F. Spronk[1,2], D. Garoz[1,2], F.A. Gilabert[1,2], E. Verboven[1], M. Kersemans[1], W. Van Paepegem[1]

[1]Department of Materials, Textiles and Chemical Engineering (MaTCh), Faculty of Engineering and Architecture, Ghent University, Tech Lane Ghent Science Park – Campus A, Technologiepark Zwijnaarde 903, B-9052 Zwijnaarde, Belgium
Email: ruben.sevenois@ugent.be, Web Page: www.composites.ugent.be
[2]SIM vzw, Technologiepark Zwijnaarde 935, B-9052 Zwijnaarde, Belgium
http://www.composites.ugent.be/

Keywords: Multiscale modeling, Constituent Property Identification, Textile composites, UD Composites, Ultrasonic Testing

Abstract
Multiscale modeling techniques for composites require input for the mechanical properties of the constituent materials (fibres and matrix). The transverse elastic properties of the fibres are often unknown because no test standard exists to determine them. One can, however, reverse engineer the fibre properties from the 3D homogenized elastic tensor of the unidirectional (UD) material. The full 3D orthotropic elasticity tensor of the UD material (carbon/epoxy) and matrix is obtained through ultrasonic insonificiation. Next, this homogenized elastic tensor is used to reverse engineer the transverse isotropic elastic tensor of the carbon fibres. To this end, 4 homogenization methods are explored: 2 analytical (Mori-Tanaka, Mori-Tanaka-Lielens), 1 semi-empirical (Chamis) and 1 finite-element (FE) (a micro-scale repetitive unit cell) homogenization method. Subsequently, the fibre properties are used to predict the elasticity tensor of UD plies with multiple fibre volume fractions. These are then used for the yarns in a meso-scale FEmodel of a plain woven material. The predicted elastic response is compared to the experimental one. The predicted and measured properties are in good agreement. It is shown that virtual identification and prediction of mechanical properties for woven plies is realistic.

1. Introduction

Regardless of whether multiscale models of fibres and matrix (for unidirectional (UD) plies) or fibre bundles and matrix (for woven composites) are based on an analytical or a Finite Element (FE) framework, the separate treatment of the constituents requires their individual mechanical properties as input. Manufacturers' datasheet only provides the stiffness and strength of the fibre in the fibre direction and the properties of the cured composite layer in the plane of the ply. However, neither the properties of pure matrix nor transverse properties of the fibres are mentioned.

The mechanical properties of the pure matrix can be obtained using standard testing methods on pure matrix samples. The direct assessment of the fiber properties in shear and transverse direction with respect to its main axis still remains challenging. Researchers often bridge the knowledge gap of unknown mechanical properties by assuming values from comparable materials out of other literature sources. Popular reference works are [1], [2]. An example of where these are used is [3]. Another

approach is to reverse engineer the constituent properties from macro-scale experimental results. This was extensively used in the recent composite failure prediction benchmark organized by the Air Force Research Laboratory [4], where several participants calibrated the constituent properties on the available experimental data.

The reverse engineering approach is promising but its usability is restricted to estimate the properties of the constituents (fibres and matrix) from microscale-based models. For fibre bundles, the variability in shape, placement and fibre volume fraction of a fibre bundle in a woven layer contains significantly more variables. Unless detailed information on the placement of the fibre bundles is available, reverse engineering the fibre bundle properties directly using a meso-scale model from the constituent material can not be done. The situation is different when it is assumed that fibre bundles are small parts of UD plies. In that case the homogenized UD ply properties can be used as input for the fibre bundles in a woven meso-model, leading to the prediction of homogenized ply properties.

In this work a complete multiscale procedure for the prediction of woven ply elastic properties starting from reverse engineered fibre and matrix properties is proposed (see figure 1). First, the 3D elastic stiffness tensor for a UD laminate is determined using contact ultrasonics. Next, the 3D elastic properties of the matrix and fibres are reverse engineered followed by a prediction of the homogenized properties of a UD ply at multiple fibre volume fractions. These predictions are used as input for the fibre bundles in a meso-scale model. The outcome of the meso-scale model is compared to the measured experimental properties of the woven laminate.

Section 2 details the experimental characterization using contact ultrasonics.. This is followed by the identification of the fibre and matrix properties from the experimental elastic tensor in Section 3 and the forward prediction of the woven material properties in Section 4. The main achievements are concluded in Section 5

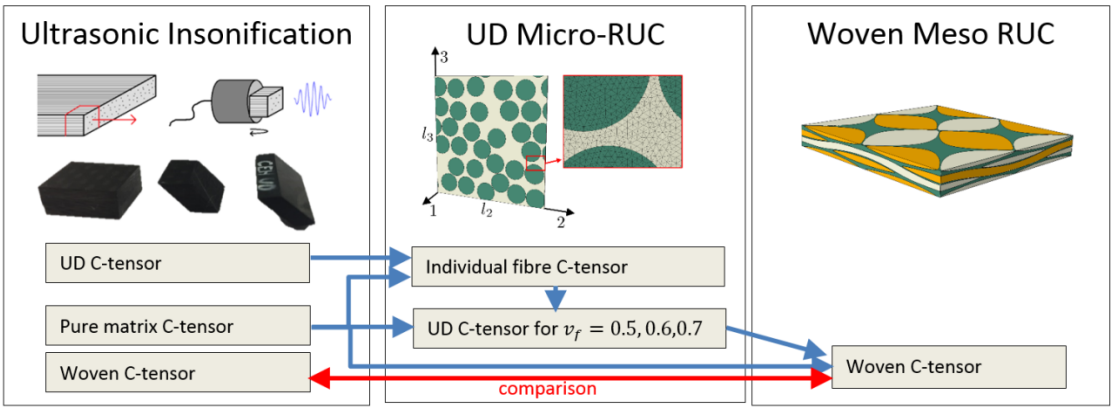

Figure 1. Procedure for the identification of fibre properties and the prediction of homogenized C-tensor for a woven composite from ultrasonic identification

2. Experimental characterization

To study the behaviour of a fibre in UD and woven configuration, it is important that the same fibres and matrix are used in both variants. Therefore, the material selected is Pyrofil TR/360 Carbon/Epoxy by Mitsubishi Chemical Corporation in both a UD (TR 360E250S) as a plain weave (TR3110 360GMP) variant.

Ultrasonic testing relies on the fact that the speed of propagation of ultrasound waves through a solid is dependent on the mechanical properties of that medium. Provided that the time-of-flight (TOF) can be recorded with sufficient accuracy, ultrasonic wave speed can be determined along different symmetry

planes, from which the elastic properties of a laminate can be derived. The contact ultrasonic pulse-echo and through-transmission methods were used to measure the phase velocity of both longitudinally and transversally polarized bulk waves along different symmetry planes. A schematic overview of the experimental setup can be found in figure 2.

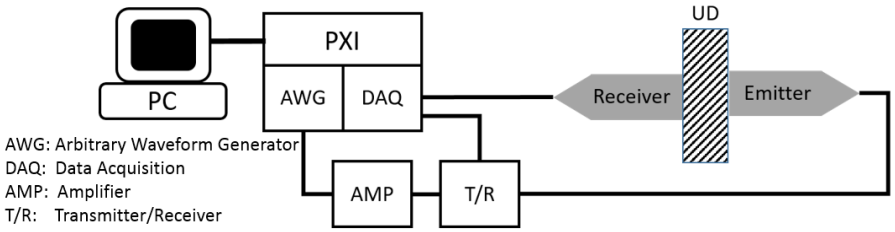

Figure 2. Schematic overview of the contact ultrasonic setup

Broadband transducers were put on opposite sides of a small piece of composite material with coupling gel such that the faces of the transducers were between 3 mm and 15 mm apart. A 2.5 MHz single-cycle sine burst with Hamming window was given as an input signal. Signals were recorded with a sampling frequency of 100 MS/s. Time-domain averaging was used in order to increase the Signal-to-Noise-Ratio (SNR) of the recorded echoes. Multiple echoes in the transmission signal were cross-correlated as well as the first echoes of the transmission and reflection signals respectively. Subsequently, the time-of-flight (TOF) of the bulk waves in the material was received from which the wave velocities could be calculated. At certain symmetry planes the Christoffel equation for orthotropic media yields a set of closed form formulas from which the elastic parameters can be determined using velocities of ultrasonic bulk waves [5]. The stiffness tensor for an orthotropic material can be written as shown below. The results of the ultrasonic characterization of the UD laminates is given in table 1.

$$\boldsymbol{C} = \begin{bmatrix} C_{11} & C_{12} & C_{13} & 0 & 0 & 0 \\ C_{12} & C_{22} & C_{23} & 0 & 0 & 0 \\ C_{13} & C_{23} & C_{33} & 0 & 0 & 0 \\ 0 & 0 & 0 & C_{44} & 0 & 0 \\ 0 & 0 & 0 & 0 & C_{55} & 0 \\ 0 & 0 & 0 & 0 & 0 & C_{66} \end{bmatrix} \tag{1}$$

A UD laminate is often assumed to behave transversely isotropic. Testing the C-tensor values for transverse isotropy with the plane of isotropy in the 23-axis, it is noted that the required relationship, $C_{23} = C_{22} - 2C_{44}$, does not seem to hold. A possible explanation can be found in the experimental C-tensor identification procedure. The combination with the large differences in Young moduli for the orthotropic directions of the laminate makes the identification procedure for the C-tensor values ill-conditioned for the entries C_{12}, C_{13} and C_{23}. Small variations in the measurements lead to large variations of the identified values.

Because the selected material models result in transversely isotropic behaviour, the values of the stiffness tensor are corrected and idealized. The small variation between longitudinal and shear coefficients, which should be equal, are recalculated as the mean value of the experimental ones, $C_{22} = C_{33} = 0.5(C_{22} + C_{33})$, $C_{55} = C_{66} = 0.5(C_{55} + C_{66})$ and $C_{12} = C_{13} = 0.5(C_{12} + C_{13})$. The value for C_{23} is recalculated according to the aforementioned relationship for transverse isotropy.

Unfortunately, the ultrasonic signals for the woven material show a large attenuation. Consequently, the elastic properties can not be obtained with sufficient confidence using this method. To provide a comparison between predicted and experimentally obtained values of the woven material, the in-plane

properties of the woven laminate are determined using standard tensile tests according to ASTM D3039 and ASTM D3518. The thus obtained elastic properties of the woven material are given in table 2.

Table 1. Ultrasonically measured stiffness tensor coefficients for the Carbon/Epoxy UD laminates

Stiffness tensor	Value (GPa)	Standard Deviation (GPa)
C_{11}	136.5000	1.04
C_{22}	12.5440	0.6
C_{33}	12.7300	0.15
C_{44}	3.2556	0.05
C_{55}	5.3987	0.28
C_{66}	5.3986	0.35
C_{12}	3.0394	0.6
C_{13}	3.0834	0.6
C_{23}	4.7347	0.27

Table 2. Ultrasonically measured elastic properties for pure matrix and tensile properties for the woven material from standard tensile testing

Stiffness tensor	Pure matrix	Plain woven C/E
E_{11}(GPa)	3.700	58.1
E_{22}(GPa)	3.700*	56.7
E_{33}(GPa)	3.700*	-
ν_{12}(-)	0.399	0.04
ν_{13}(-)	0.399*	-
ν_{23}(-)	0.399*	-
G_{12}(GPa)	1.322**	3.6
G_{13}(GPa)	1.322**	-
G_{23}(GPa)	1.322**	-

*isotropic assumption; ** $G = E/(2(1+\nu))$

3. IDENTIFICATION OF FIBER AND MATRIX CONSTITUENT PROPERTIES

The linear elastic properties of the individual fibres are determined from the stiffness tensor of the UD ply, $\boldsymbol{C^{UD}}$, and pure matrix, $\boldsymbol{C^{m}}$, through reverse engineering using a homogenization method. The results from four different homogenization methods, two analytical methods, Mori-Tanaka (MT) [6] and Mori-Tanaka-Lielen (MTL) [7]; one semi-empirical method, Chamis (CHAM) [8] and one FE Representative Volume Element (RVE) homogenization model are compared.

To do this with a micro-mechanical model the homogenized stiffness tensor of a UD laminate $\widetilde{\boldsymbol{C}}^{UD}$ is written as a function of the stiffness tensors of the matrix $\boldsymbol{C}^{m}$ and fibers $\boldsymbol{C}^{f}$:

$$\widetilde{\boldsymbol{C}}^{UD} = h(\boldsymbol{C}^{f}, \boldsymbol{C}^{m}) \tag{2}$$

where the function h takes into account the micro-structure of the UD laminate. For the four material models, unfortunately h cannot be inverted mathematically to determine $\boldsymbol{C}^{f}$ exactly. Therefore the secant method is used to determine the properties of $\boldsymbol{C}^{f}$. From two initial guesses of the fibre stiffness

tensor the homogenized stiffness tensor is calculated twice. Using both estimations and the target experimental value for the homogenized tensor a new guess for the fibre tensor is then obtained by:

$$\left[C_{mn}^{f}\right]^{i+1} = \left[C_{mn}^{f}\right]^{i} - [\Phi_{\mathrm{mn}}]^{i} \frac{\left[C_{mn}^{f}\right]^{i} - \left[C_{mn}^{f}\right]^{i-1}}{[\Phi_{\mathrm{mn}}]^{i} - [\Phi_{\mathrm{mn}}]^{i-1}} \tag{3}$$

Where $[\boldsymbol{\Phi}]^{i}$ is the residual stiffness tensor calculated as the differences between $\boldsymbol{C}^{UD.}$ and $\widetilde{\boldsymbol{C}}^{UD}$, which are the experimental and the homogenized UD stiffness tensors, respectively. The procedure is repeated with the new value for the fibre stiffness tensor until the residual stiffness coefficient are below a tolerance of 10^{-6} to reach a precision of 4 significant figures.

In terms of microstructural properties the MT, MTL and CHAM models assume an idealized fibre placement with fibres as infinitely long cylinders in an infinite matrix. The geometry of the periodic RVE model is given by a cuboid composed of a random distribution of fibers parallel to direction 1, see figure 3. The radius of the fibers is known, $r^f = 3.6\,\mu m$, and the volume fraction is fixed, $v_f = 0.6$. The dimensions of the transverse section l_2 and l_3 are calculated from the number of fibers n^f, r^f and v_f assuming an initial hexagonal package. l_1 is, in this work, determined by the element size. To minimize the computational effort this is chosen as one layer of elements.

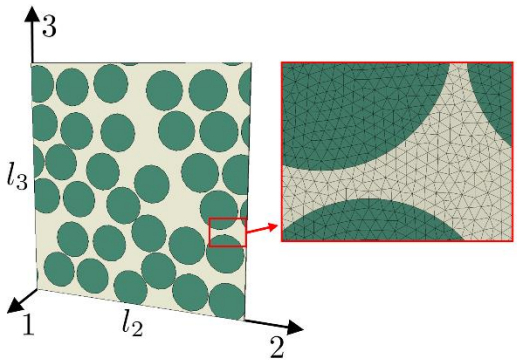

Figure 3. RVE with 30 fibers and mesh detail.

The random distribution of fibers is generated with a simple collision model [9] keeping v_f constant. Different RVEs with a total of 30 fibers are generated. The geometry is dicretized using wedge elements with 6 nodes and 2 integration points (C3D6 Abaqus), see figure 3. It is verified that a global element size of 0.03 mm ensures converge of the homogenized elastic properties for the RVE. Consistent Periodic Boundary Conditions (PBCs) are applied between the three pairs of parallel faces of the geometry [10].

The homogenized elastic properties are obtained by imposing 6 load cases, three longitudinal and three shear strains, as macro-strains via the PBCs. Weighted volume averaging of the stress field in combination with the macro-strains results in the homogenized stiffness tensor of the UD laminate. To take into account the randomness distribution of fibers in the RVE, the fiber properties shown are an average of the properties from 3 different configurations. The small dispersion warrants that the RVE with 30 fiber contains sufficient fibres to give representative and reliable values.

For all models, the carbon fibers are assumed to have transversely isotropic properties. They exhibit the same symmetry about the three principal coordinates planes as for the UD laminate. This results in 5 independent coefficients to be determined for the fibre stiffness tensor $\boldsymbol{C}^{f}$. Table 3 shows the fiber properties from the iterative identification resulting from the four formulations.

Table 3. Fibre constituent properties for different micro-homogenizaton methods

Stiffness tensor	Mori-Tanaka	Mori-Tanaka-Lielen	Chamis	FE-RVE
E_{11}(GPa)	223.101	222.350	223.366	223.300
E_{22}(GPa)	20.764	14.776	18.107	18.365
E_{33}(GPa)	20.764	14.776	18.107	18.365
ν_{12}(-)	0.018	0.054	0.006	0.022
ν_{13}(-)	0.018	0.054	0.006	0.022
ν_{23}(-)	0.182	0.366	0.599	0.269
G_{12}(GPa)	>1000	14.619	51.951	36.898
G_{13}(GPa)	>1000	14.619	51.951	36.898
G_{23}(GPa)	8.781	5.407	5.661	7.241

Several other investigations on the accuracy of the methods used show that MT gives homogenized stiffness values above the experimental ones while MTL underestimates the homogenized stiffness values. Therefore the identified fibre properties by MT can be taken as upper bound for the stiffness and lower bounds for the Poisson's ratio. Instead, MTL behaves reversely. The identified properties can be taken as lower bounds for stiffness and upper bound for Poisson's ratio. This is confirmed by the properties from FE-RVE, which are between MT and MTL. A similar observation is seen for CHAM's prediction, except for the Poisson ratio. Also, MT reports unrealistically high shear stiffnesses G_{12} and G_{13}. This is a consequence of the assumption of diluted inclusions in a continuous media which is not completely correct for the assumed volume fraction of 60%. For all the used micro-structural models, the fibre Poisson's ratio ν_{12} of the fibers is small compared with the usual reported value of around 0.2 [11]. This is a direct effect of the small experimentally obtained value of the UD laminate $\nu_{12} = 0.176$.

With the identified material properties of each constituent, the properties of UD plies with different volume fractions v_f are calculated via FE. The UD laminate properties for v_f between 50% and 90% are calculated using the 30 fibre-RVE. The results are used as input for the yarn bundles in the woven meso-scale RVE.

4. PREDICTION OF WOVEN ELASTIC PROPERTIES

The prediction of the mechanical properties of a woven ply is carried out using a RUC at the meso-scale. Knowledge about the geometrical arrangement of the fibre bundles in the laminate has been obtained by the authors in a previous work[3].

In [3], a new method for the construction of a meso RUC was proposed. The Measurement Enhanced Shape Identification (MESI) method uses a general and periodic form of the superelliptic function to provide smoothly varying closed yarn regions. The resulting RUC is a 2-ply RUC (figure 4), where the plies are nested out-of-phase to achieve a correct and realistic yarn-matrix volume fraction. A consequence of the variable cross section is that the fibre volume fraction of the yarns varies accordingly. This is shown for the warp yarns in steps of 5% v_f in figure 4.

The meso-scale RUC is meshed with 43,520 C3D20 hexahedrals in the yarns and 532,875 C3D10 tetrahedrals in the matrix resulting in a total of 1,235,692 nodes. A mesh convergence study confirmed that this is not only sufficient to achieve convergence for the homogenized elastic properties, but also in the internal yarn and matrix stress fields. Since hexahedrals and tetrahedrals are incompatible elements, yarns and matrix are connected using a surface tie formulation. The PBC and homogenization procedure is the same as used for the micro-scale RVE. The predicted ply properties from the meso-scale RUC are given in table 4 together with a comparison with the measured properties from the woven material.

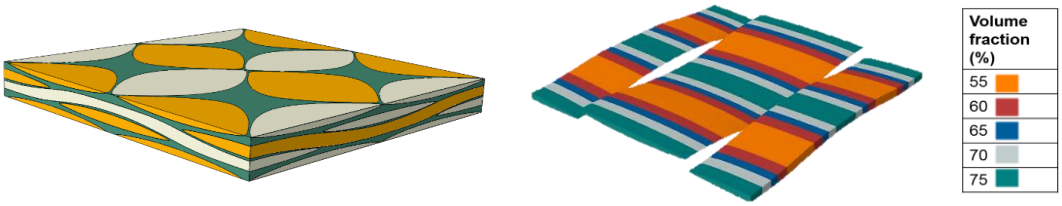

Figure 4. Meso-RVE Geometry and fibre volume fraction distribution in warp yarns

Between the meso-scale RVE and the experimental values, there is a small variation in the Young's moduli. Larger differences are seen for the shear modulus G_{12} that results 50% higher than the experimental one. The Poisson's ratio agrees well. The reason for the large difference in shear modulus is currently unknown. The authors suspect that a difference in behaviour of the UD material due to the high strain rate excerted during the ultrasonic measurement in combination with rate dependency of the matrix material might overstimate the fibre properties in shear direction. As a consequence, the experimental work from the tensile tests on the woven material results in a lower shear stiffness than the "high strain rate" prediction by the woven Meso-RVE.

Table 4. Comparison experimental properties and meso-RVE properties of woven material

Stiffness tensor	Plain woven C/E	Meso-RVE
E_{11}(GPa)	58.1	60.0
E_{22}(GPa)	56.7	59.3
E_{33}(GPa)	-	10.8
ν_{12}(-)	0.04	0.05
ν_{13}(-)	-	0.41
ν_{23}(-)	-	0.41
G_{12}(GPa)	3.6	5.1
G_{13}(GPa)	-	3.3
G_{23}(GPa)	-	3.3

5. CONCLUSION

In this work a multiscale framework to predict the elasticity tensor of carbon fibres and woven carbon composites by ultrasonic insonification is presented.

An important aspect for the identification of fibre properties is the ability to obtain the 3D mechanical properties of the UD laminate. This was done using the ultrasonic testing of small cubes of UD and pure matrix material. It was not possible to obtain 3D mechanical properties of the woven material due to large attenuation of the ultrasonic signals. Alternatively, the in-plane properties of the woven material were determined using standard tensile tests.

Identification of the fibre properties from the measured UD ply properties was done with 2 analytical, 1 semi-analtyical and 1 FE-RVE model. It is shown that, depending on the homogenization method, the identified properties can vary considerably. Unfortunately, there are not direct experimental measurements of the full set of elastic coefficients of individual fibres. This prevents to assess which model is the most accurate. The MT and MTL models were, in other investigations, identified as the models providing the boundaries within which the fibre properties should lie. It is shown here that there is a negligible difference between MTL or the FE-RVE models. Except for the in-plane shear modulus,

the predicted properties by the woven RVE agree well with the experimentally obtained values. The disagreement with the in-plane shear stiffness, G_{12}, is large and requires further research.

Although some work remains, two conclusions are drawn from this work: (i) backward identification of fibre properties from 3D mechanical properties of UD laminates produces acceptable values for single fibre properties and (ii) the multiscale model of woven properties from fibre and matrix properties leads to good predictions of the ply mechanical properties.

Acknowledgments

This work is funded by SBO project "M3Strength", MacroModelMat (M3) research program by SIM (Strategic Initiative Materials in Flanders) and VLAIO (Flemish government agency Flanders Innovation & Entrepreneurship).

References

[1] A. Arteiro, G. Catalanotti, A. R. Melro, P. Linde, and P. P. Camanho, "Micro-mechanical analysis of the in situ effect in polymer composite laminates," *Compos. Struct.*, vol. 116, pp. 827–840, Sep. 2014.

[2] P. D. Soden, M. J. Hinton, and A. S. Kaddour, "Lamina properties, lay-up configurations and loading conditions for a range of fibre-reinforced composite laminates," *Compos. Sci. Technol.*, vol. 58, no. 7, pp. 1011–1022, Jul. 1998.

[3] R. D. B. Sevenois, D. Garoz, F. A. Gilabert, S. W. F. Spronk, S. Fonteyn, M. Heyndrickx, L. Pyl, D. Van Hemelrijck, J. Degrieck, and W. Van Paepegem, "Avoiding interpenetrations and the importance of nesting in analytic geometry construction for Representative Unit Cells of woven composite laminates," *Compos. Sci. Technol.*, vol. 136, pp. 119–132, Nov. 2016.

[4] S. B. Clay and S. P. Engelstad, "Benchmarking of composite progressive damage analysis methods: The background," 2017.

[5] W. C. Van Buskirk, S. C. Cowin, and R. N. Ward, "Ultrasonic measurement of orthotropic elastic constants of bovine femoral bone," *J. Biomech. Eng.*, vol. 103, no. 2, pp. 67–72, 1981.

[6] T. Mori and K. Tanaka, "Average stress in matrix and average elastic energy of materials with misfitting inclusions," *Acta Metall.*, vol. 21, no. 5, pp. 571–574, 1973.

[7] G. Lielens, P. Pirotte, A. Couniot, F. Dupret, and R. Keunings, "Prediction of thermo-mechanical properties for compression moulded composites," *Compos. Part A Appl. Sci. Manuf.*, vol. 29, no. 1, pp. 63–70, 1998.

[8] C. C. Chamis, "Micromechanics strength theories. [for unidirectional composites]," 1974.

[9] B. D. Lubachevsky and F. H. Stillinger, "Geometric properties of random disk packings," *J. Stat. Phys.*, vol. 60, no. 5–6, pp. 561–583, Sep. 1990.

[10] D. Garoz, F. A. Gilabert, R. D. B. Sevenois, S. W. F. Spronk, and W. Van Paepegem, "Consistent Application of Periodic Boundary Conditions in Implicit and Explicit Finite Element Simulations of Damage," *Compos. Struct.*, p. (Submitted), 2018.

[11] D. M. Blackketter, D. Upadhyaya, and T. R. King, "Micromechanics Prediction of the Transverse Tensile Strength of Carbon Fiber / Epoxy Composites : The Influence of the Matrix and Interface," *Polym. Compos.*, vol. 14, no. 5, pp. 437–446, 1993.